Cerebral Cortex July 2011;21:1613–1626
doi:10.1093/cercor/bhq223
Advance Access publication December 1, 2010

Conserved Subcortical and Divergent Cortical Expression of Proteins Encoded by Orthologs of the Autism Risk Gene MET

Matthew C. Judson[1], David G. Amaral[2] and Pat Levitt[3,4,5]

[1]Graduate Program in Neuroscience, Vanderbilt University Medical Center, Nashville, TN 37203, USA, [2]The MIND Institute and the Department of Psychiatry and Behavioral Sciences, University of California, Davis, CA 95817, USA, [3]Vanderbilt Kennedy Center for Research on Human Development and [4]Department of Pharmacology, Vanderbilt University Medical Center, Nashville, TN 37203, USA and [5]Zilkha Neurogenetic Institute and the Department of Cell and Neurobiology, Keck School of Medicine, University of Southern California, Los Angeles, CA 90089, USA

Address correspondence to email: matthew_judson@med.unc.edu.

Met receptor tyrosine kinase signaling regulates the growth and development of axons and may contribute to the wiring of cortical and limbic circuits in the rodent forebrain. Whether the orthologous MET receptor functions similarly in the developing primate forebrain is not known but is of considerable interest considering the association of variant MET alleles with social and communication phenotypes in autism. To begin addressing this question, we compared Met/MET protein expression in the developing mouse and rhesus macaque forebrain. There was a strong temporal conservation of expression during the time of rapid axon development and the onset of robust synapse formation. Expression patterns of Met/MET in limbic-related structures were almost identical between species. In marked contrast, there was highly divergent expression in the neocortex. In mouse, Met was broadly distributed throughout neocortex. In the macaque, robust MET expression was largely restricted to the posterior cingulate, inferior temporal, posterior parietal, and visual cortices, including face processing regions. The pattern is consistent with the importance of vision in the social repertoire of the primate. Collectively, these data suggest a conserved developmental function of the MET receptor in wiring together limbic and neocortical circuits that facilitate species-appropriate responses, including social behavior.

Keywords: circuitry, HGF, neocortex, social, vision

Introduction

Current etiological theories of autism spectrum disorders (ASDs), defined in part by deficits in social interaction and communication, are based on the concept of developmental disruptions in forebrain connectivity (Frith 2004; Geschwind and Levitt 2007; Levy 2007). Evidence supporting these theories has largely come from genetic susceptibility, correlated clinical phenotypes, and functional imaging studies. The latter have revealed altered patterns of brain activity and synchronization in individuals with ASD during social information processing and communication tasks (Just et al. 2004; Koshino et al. 2008). However, a mechanistic understanding of the development of aberrant social circuitry is currently limited.

One approach to elucidating etiological mechanisms of ASD is to study the developmental functions of associated variant genes. Genetic studies of ASD have revealed copy number variations (Marshall et al. 2008), rare mutations, and the association of 2 common allelic variants (rs1858830-C and rs38845-A) of the *MET* receptor tyrosine kinase gene in 4 family cohorts (Campbell et al. 2006; Campbell et al. 2008; Jackson et al. 2009; Sousa et al. 2009). Moreover, an enriched association of the rs1858830-C allele specifically with social and communication phenotypes of ASD was recently demonstrated (Campbell et al. 2010). Because Met signaling in vitro potentiates axon outgrowth, dendritogenesis, and synaptogenesis (Ebens et al. 1996; Gutierrez et al. 2004; Madhavan and Peng 2006; Tyndall and Walikonis 2006; Nakano et al. 2007), a basic mechanistic hypothesis relating *MET* gene function and ASD risk has emerged: Decreased MET protein expression during development increases the risk of ASD-relevant circuit miswiring. As for most ASD-risk genes, the details of spatial and temporal patterns of Met expression have been described solely in the rodent. Our recent study in the mouse reported a restricted temporal expression of Met during the onset and peak of synaptogenesis in subcortical limbic structures, as well as broad distribution throughout the neocortex (Judson et al. 2009). It is not known how this translates to relevant at-risk primate circuitry.

Mammalian conspecifics, including primates, exchange information concerning fitness, mating status, and other factors influencing individual or group survival through various sensory modalities. Stereotyped forebrain circuitry has evolved to support the cognitive processing that underlies this conserved social behavior. For example, circuits involving the hippocampal formation and mammillary nuclei facilitate the encoding of socially relevant spatial cues and social recognition (Sanchez-Andrade et al. 2005; Steckler et al. 1998). The emotional quality of social stimuli is processed by the amygdala in all mammalian species (Phelps and LeDoux 2005). The input pathways that route social information to these conserved cognitive circuits, however, are divergent across mammalian taxa, reflecting the sensory world of each class of animals (Hauser 1996). Primates, for instance, communicate primarily by issuing physical gestures and vocalizations, the receipt of which requires visual and auditory system function, respectively. In contrast, rodents depend more heavily on olfaction and somatosensation to communicate. Appropriate social behavior, therefore, depends on the wiring together of relevant sensory and cognitive circuitry during development, which may differ across species. In an attempt to understand the circuits that may be at greatest risk in ASD due to the allelic MET variants identified in multiple genetic studies, we specifically compare Met receptor expression in the mouse forebrain with that of its ortholog, MET, in the macaque forebrain across corresponding periods of development.

Materials and Methods

Preparation of Fixed Brain Sections

Wild-type C57BL/6J mice were either purchased from the Jackson Laboratory or harvested from $Emx1^{cre}/Met^{fx/+}$ × $Emx1^{+}/Met^{fx/fx}$

matings using previously described mouse husbandry and genotyping strategies (Judson et al. 2009). In the latter case, mice with a $Met^{fx/fx}$ or $Met^{fx/+}$ genotype were considered wild type if they did not have Cre recombinase knocked-in to the 3′ untranslated region of either Emx1 allele. Mice aged between postnatal (P) day 0 and 21 ($N > 3$ each age) were deeply anesthetized with sodium pentobarbital (60 mg/kg intraperitoneally) prior to transcardial perfusion with room temperature phosphate-buffered 4% paraformaldehyde (pH 7.3) containing 1.3% L-lysine and 0.24% sodium periodate. After postfixation overnight at 4 °C, brains were cryoprotected via sequential 12-h incubations in 10%, 20%, and 30% sucrose in phosphate-buffered saline (PBS), pH 7.5. Fixed brains were then sectioned as previously described (Judson et al. 2009). Briefly, P0 brains were sectioned at 20 μM with a cryostat, and P7–P21 brains were sectioned at 40 μM with a freezing sliding microtome (Leica). Prior to immunohistochemical processing, P0 sections were stored at –80 °C on gelatin-coated slides and P7–P21 sections were stored at –20 °C, free-floating in a cryopreservative solution.

Pre- (i.e., gestational day [GD] 100 and 150) and postnatal (i.e., P21) rhesus monkey brains ($N = 2$ each age) were obtained at the California National Primate Research Center. Animals were deeply anesthetized with sodium pentobarbital (50 mg/kg intravenously, Fatal-Plus, Vortech Pharmaceuticals) and perfused transcardially with ice-cold 1% and 4% paraformaldehyde in 0.1 M phosphate buffer (pH 7.4) following a standard laboratory protocol (Lavenex et al. 2009). The brains were postfixed for 6 h in the same fixative, cryoprotected in 10% and 20% glycerol solutions in 0.1 M phosphate buffer (pH 7.4, for 24 and 72 h respectively), rapidly frozen in isopentane and stored at –70 °C until sectioning. Sections were cut at 30 μm on a freezing sliding microtome and processed immunohistochemically as described below.

All research procedures using mice and macaques conformed to National Institutes of Health guidelines and were approved by the Institutional Animal Care and Use Committees at Vanderbilt University and the University of California at Davis, respectively. All efforts were made to minimize animal suffering and to reduce the number of animals used.

Met/MET Immunohistochemistry

Two different monoclonal antibodies were used for Met/MET immunohistochemical study: 1) mouse anti-Met (Met, B-2; sc-8057; Lot No. C2807; Santa Cruz Biotechnology) and 2) mouse anti-Met (Met, 25H2; #3127; Lot No. 3; Cell Signaling Technology). Met immunohistochemistry was performed as previously described (Judson et al. 2009). Briefly, free-floating mouse or macaque brain sections were rinsed several times in PBS before the following blocking procedures were applied: 1) 5 min in 0.3% H_20_2 in methanol, 2) 25 min in 0.1 M Tris-glycine (pH 7.4), and 3) 25 min in Blotto-T (4% Carnation dried milk in PBS containing 0.2% Triton-X-100). PBS rinses preceded both the Tris-glycine and the Blotto-T blocking steps. For mouse tissue, an additional 1.5-h incubation in unlabeled donkey anti-mouse IgG (Fab; Jackson Immunoresearch) was performed immediately before the Blotto-T step in order to block endogenous immunoglobulin. After blocking, brain sections were incubated in primary anti-Met antibodies for 48 h at 4 °C. Specifically, sections were incubated in either 1:250 anti-Met (Santa Cruz sc-8057, mouse sections only) or 1:400 anti-Met (Cell Signaling #3127, some mouse sections and all macaque sections) diluted in Blotto-T. Following washes in Blotto-T, sections were then incubated for 1 h at room temperature in 1:1000 biotin-SP-conjugated donkey anti-mouse IgG (Jackson Immunoresearch) diluted in Blotto-T. Sections were then rinsed several times in PBS and processed by the ABC Elite histochemical method (Vector). Met-specific antibody complexes were visualized by incubating the sections for 2–4 min at room temperature in 0.05% 3′3′-diaminobenzidine with 0.015% H_20_2.

Cross-species Use of Antibodies

We examined the cross-species reactivity of the 2 commercially available mouse monoclonal antibodies used to immunohistochemically label mouse Met protein and homologous monkey MET protein in the present study. These antibodies were generated against synthetic peptides corresponding to highly conserved intracellular domains of the mouse (Santa Cruz #8057; immunogen: amino acids 1330–1379 [NCBI No. NP 032617, 86% sequence identity with human]) and human (Cell Signaling #3127; immunogen: amino acids 1228–1243 [NCBI No. AAA59591, 100% sequence identity with mouse]) receptors. They exhibited remarkably high species cross-reactivity when substituted for each other in a previously described immunohistochemical staining protocol (see "Met/MET immunohistochemistry" subsection of Materials and Methods [Judson et al. 2009]). Cell Signaling #3127, which specifically recognizes MET on western blots prepared from GD152 macaque whole-brain lysates (Supplementary Fig. 1E), yielded staining patterns in somatosensory cortex (Supplementary Fig. 1B) and hippocampus (Supplementary Fig. 1D) that were indistinguishable from those produced by staining with the Santa Cruz #8057 antibody in comparable brain regions (Supplementary Fig. 1A,C) in P7 mice. Note also that these antibodies were tested previously in the *Met* conditional null mouse and showed minimal to no immunostaining in tissue sections (Judson et al. 2009).

Digital Illustrations

Microscopy was performed with the aid of an Axioplan II microscope (Zeiss), and micrographs were acquired with a Zeiss AxioCam HRc camera (Zeiss) in Axiovision 4.1 software (Zeiss). Low-magnification montage images of macaque brain sections were prepared and linearly adjusted for brightness and contrast using Adobe Photoshop (Version 7.0, Adobe). No other image alterations other than resizing were performed. All figures were prepared digitally in Microsoft Office Powerpoint 2003.

Results

Conserved Temporal Patterns of Met/MET Expression

Beginning in late neurogenesis and persisting through the first postnatal week in the mouse, neocortical Met expression increases dramatically, and the receptor is readily detected by immunohistochemical methods first in axon tracts, and later in the neuropil, of the neocortex (Judson et al. 2009). By the end of the second postnatal week, corresponding with a winding down of axonal outgrowth and the beginning of the peak synaptogenic period, neocortical Met expression begins to decline. By P21, Met is detected only sparsely in the neocortical neuropil (Judson et al. 2009).

To address the possibility of an evolutionarily conserved expression pattern for the orthologous MET receptor during development in the primate forebrain, we performed MET immunohistochemistry at corresponding developmental timepoints in the macaque. These included GD100 during late neocortical neurogenesis (Rakic 1974) and GD150 and postnatal (P) day 21, which mark the rise and plateau, respectively, of the peak synaptogenic phase in the macaque monkey (Bourgeois and Rakic 1993; Bourgeois et al. 1994). MET immunohistochemical staining in the GD100 macaque was restricted to select regions of the neocortex. Here, receptor localization was evident in outgrowing axons of projection neurons and, though more broadly distributed across the radial dimension of the cortex, closely resembled the pattern of Met labeling observed in the mouse at P0 (Fig. 1*A,E*). At the cellular level by GD150, the pattern of MET labeling expanded to include the neocortical neuropil in a manner similar to that observed in the mouse at P7. In both species, the punctate staining within the neuropil yielded salient patterns consistent with membrane localization of the protein, including images of cell bodies in negative relief, a noticeable increase in marginal zone labeling, and a relative paucity of layer IV labeling (Fig. 1*B,F* and *C,G*). Whereas cortical neuropil labeling increased toward the onset of peak synaptogenesis, staining in

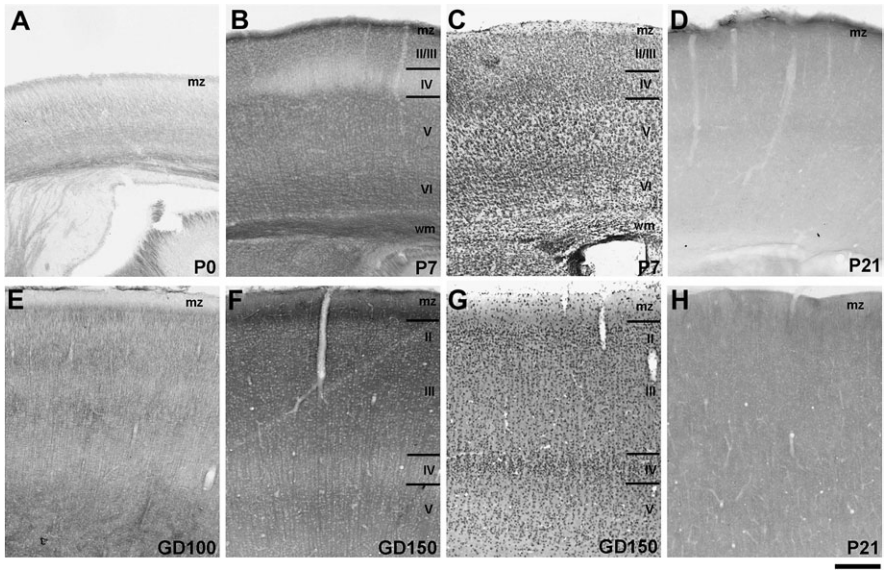

Figure 1. Conserved temporal patterns of Met/MET expression in the neocortex. Differential interference contrast photomicrographs of coronal brain sections illustrate Met/MET immunohistochemistry in mouse barrel cortex and macaque inferotemporal cortex. Labeling is predominantly seen in the outgrowing axons of cortical projection neurons in the cortex of the P0 mouse (*A*) and GD100 macaque (*E*). During axon collateralization and the onset of synaptogenesis, Met/MET labeling is readily observed in neuropil compartments in both species (*B*, *F*). Nissl staining in matched cortical regions (*C*, *G*) reveals that expression is especially heavy in the marginal zone (mz) and relatively sparse in layer IV at this developmental stage. By 3 weeks of age (*D*, *H*), early periods of axon wiring have past in both mice and macaques, corresponding with drastically decreased immunohistochemical detection of Met/MET. Scale bar = 138 μM for all images.

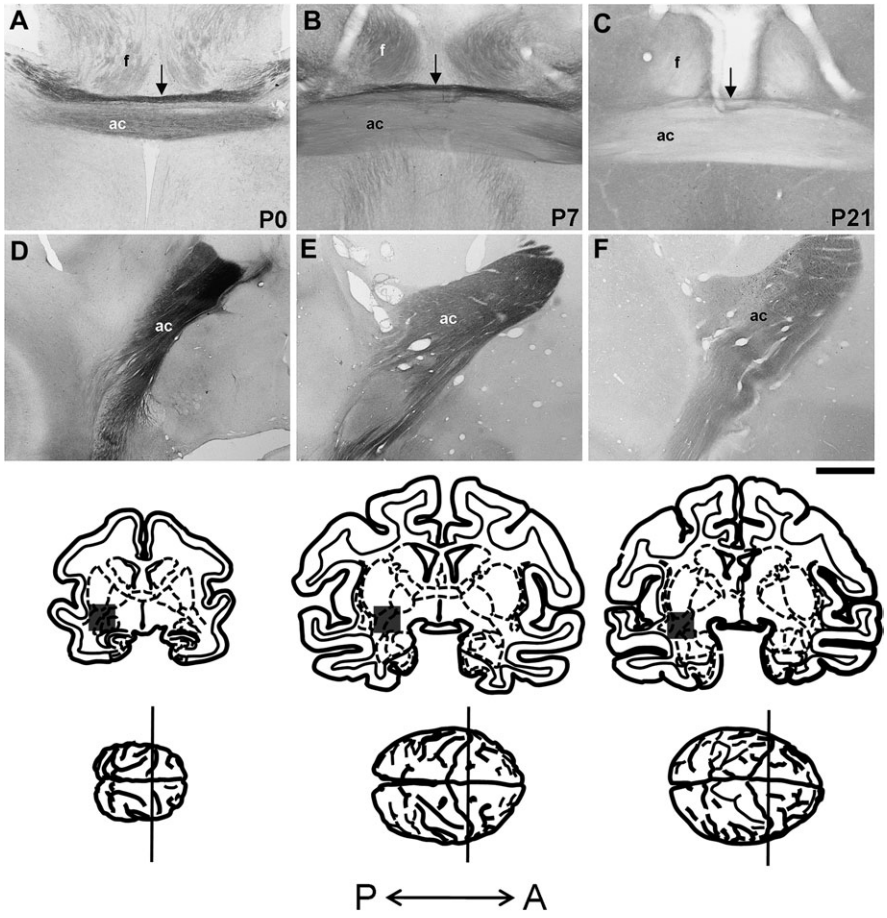

Figure 2. Conserved temporal patterns of Met/MET expression in the anterior commissure. Differential interference contrast photomicrographs illustrate Met/MET immunohistochemistry in mouse and macaque coronal brain sections during development. In both the mouse (*A*) and macaque (*D*), intense Met/MET staining of corticofugal axons within the anterior commissure (ac) is observed at time-points just after the end of cortical neurogenesis. Axon staining within this structure gradually decreases in intensity throughout perinatal/early postnatal development in both species (mouse *B* and *C*; macaque *E* and *F*). The body of the ac, located just inferior to a commissural division of the ST (arrows), is depicted in mouse panels (*A*–*C*), whereas the temporal limb of the ac is depicted in macaque panels *D*–*F*. The boxed region in schematized macaque brain sections corresponds to the photomicrograph directly above. The posteroanterior (P← →A) position of macaque sections is indicated in schematized dorsal views of the brain. f, fornix. Scale bar = 275 μM for (*A*–*C*); 1.1 mm for (*D*–*F*).

forebrain axon tracts that carry corticocortically projecting axons, such as the anterior commissure, concomitantly declined (Fig. 2*A*,*B* and *D*,*E*).

There were comparable temporal dynamics of Met/MET expression within the terminal fields of subcortically projecting neocortical axons. In the mouse at P0, Met was expressed in developing principle axon tracts including the internal capsule (Fig. 3*A*; Supplementary Fig. 2A,B), which contains corticofugal projections to the thalamus and striatum. However, in neither the mouse nor the macaque was neuropil labeling apparent in presumed corticothalamic (Fig. 3*A*,*B*,*E*,*F*) or corticostriatal (Supplementaatry Fig. 2A,B,E,F) axon terminal fields at this developmental stage. Robust Met/MET staining in the thalamic (Fig. 3*C*,*D*,*G*,*H*) and striatal (Supplementary Fig. 2C,D,G,H) neuropil became evident by P7 in the mouse and GD150 in the macaque, and, as shown in high-magnification images (Figs 1*B*,*E* and 3*D*,*H*; Supplemental Fig. 2D,H), the pattern of labeling was reminiscent of that seen in the neocortex at this same stage of development. Finally, as in the mouse, immunohistochemical detection of MET was dramatically reduced in major forebrain axon tracts and neocortical and subcortical axon terminal fields at P21, approaching the plateau of the peak synaptogenic period (Figs 1*D*,*H* and 2*C*,*F*).

Expression of Met/MET in the Limbic System

In both the P7 mouse and GD150 macaque, Met/MET staining was evident throughout the anteroposterior extent of the amygdala, but the intensity of the staining varied within individual amygdaloid nuclei at each level. We observed robust neuropil staining in the P7 mouse amygdala in the nucleus of the lateral olfactory tract, anteriorly (Fig. 4*A*), and the posterior cortical nucleus, posteriorly (Fig. 4*C*). These 2 nuclei of the amygdala, as per (Swanson and Petrovich 1998), were apparently devoid of labeling in the macaque (data not shown). More moderate neuropil staining in the lateral (L), basal (B), and accessory basal (AB) nuclei at intermediate levels of the amygdala was generally conserved between the 2 species (Fig. 4*B*,*D*–*F*). There was a conserved L (moderate) to AB (low) gradient of Met/MET staining across these contiguous deep amygdaloid nuclei, which was most salient in the macaque at anterior and intermediate anteroposterior levels (Fig. 4*D*–*F*). Moreover, at intermediate anteroposterior levels of the macaque (Fig. 4*E*), staining was specifically localized to a dorsolateral subdivision of L and the dorsal subdivision of B. These patterns are largely consistent with the known projections from inferotemporal cortex to the amygdala in the macaque monkey (Stefanacci et al. 1996; Stefanacci and Amaral 2002).

Amygdaloid neurons in both species expressed Met/MET in their efferent projecting axons. The stria terminalis (ST), which is the principle tract carrying amygdalofugal axons within the mammalian forebrain, was densely labeled in the mouse at P7 (Supplementary Fig. 3B; Fig. 6*A*). We observed MET labeling of relatively modest intensity within this axon tract in the GD150 macaque (Supplementary Fig. 3E). In both species, it was evident that only select populations of amygdalofugal axons are stained (Supplementary Fig. 3B,E). Moreover, decrimental staining was observed within these axon subpopulations with increasing developmental age (Supplementary Fig. 3A–C and D–F), mirroring the conserved temporal pattern of expression for corticocortical and corticofugal axon tracts. A minor subset of

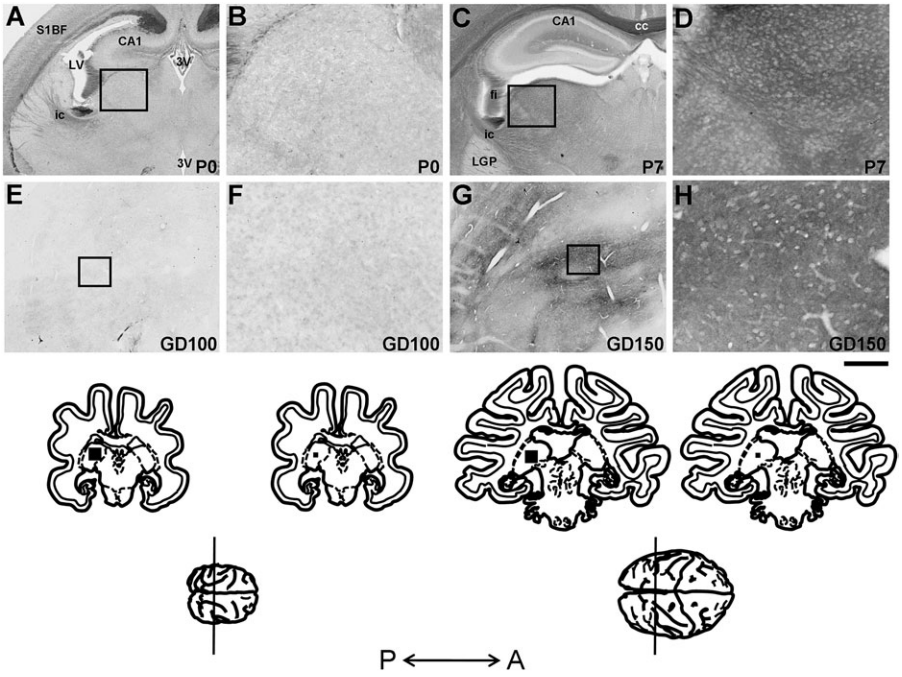

Figure 3. Conserved temporal patterns of Met/MET expression in the corticothalamic projection. Differential interference contrast photomicrographs illustrate Met/MET immunohistochemistry in coronal brain sections during development. Axonal Met staining is evident in the internal capsule (ic, *A*) but not corticothalamic terminal fields (*B*, boxed region in *A*) in the dorsal thalamus in the P0 mouse. A similar pattern of expression is observed in low- (*E*) and high-magnification (*F*) images of the pulvinar in the GD100 macaque. Corresponding images in the P7 mouse (*C* and *D*) and GD150 macaque (*G* and *H*) show dramatically increased Met labeling of the thalamic neuropil, concurrent with robust periods of corticothalamic terminal arborization in each species. The boxed region in schematized macaque brain sections corresponds to the photomicrograph directly above. The posteroanterior (P⟵⟶A) position of macaque sections is indicated in schematized dorsal views of the brain. 3V, third ventricle; CA1, cornu ammonis 1 of hippocampus; cc, corpus callosum; fi, fimbria of hippocampus; LGP, lateral globus pallidus; S1BF, barrel field of primary somatosensory cortex. Scale bar = 550 μM for (*A*) and (*C*); 825 μM for (*E*) and (*G*); 138 μM for (*B*), (*D*), (*F*), and (*H*).

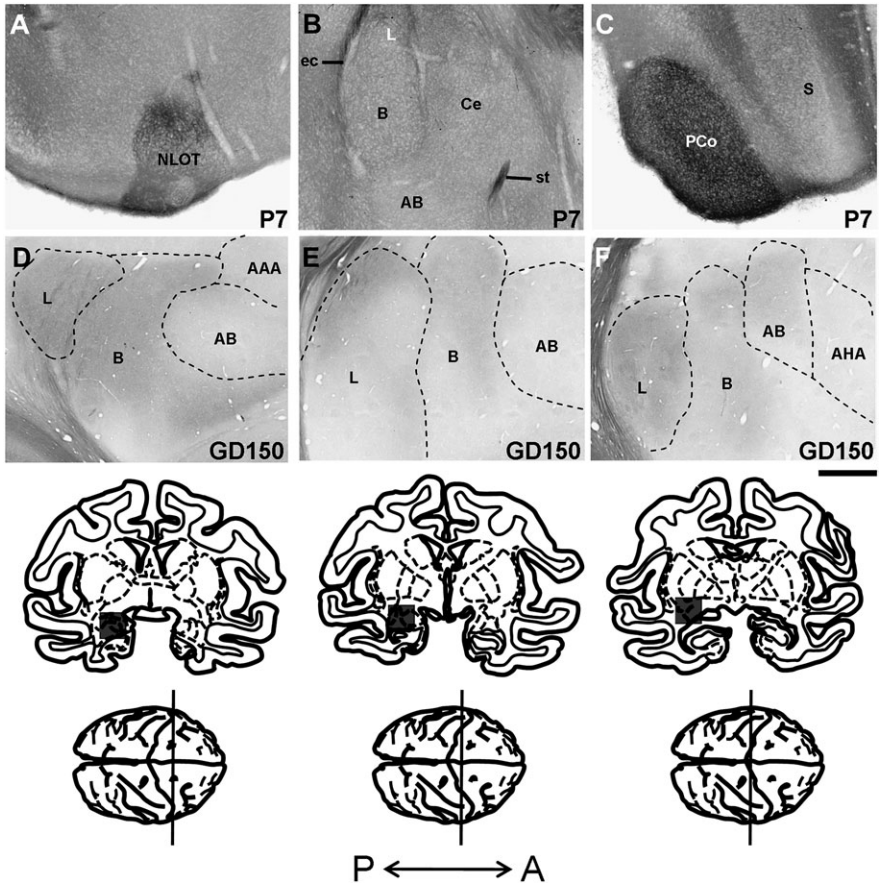

Figure 4. Conserved Met/Met expression in amygdaloid afferents. Differential interference contrast photomicrographs illustrate Met/MET immunohistochemistry at various anteroposterior levels of the amygdala in coronal brain sections from the P7 mouse and GD150 macaque. Though Met expression is widespread in the mouse amygdala during axon collateralization, the nucleus of the lateral olfactory tract (NLOT, *A*) and the posterior cortical nucleus (PCo, *C*) exhibit exceptionally heavy Met labeling. More moderate labeling in the basolateral complex is greatest in the lateral (L) nucleus, and of decreased intensity in the basal (*B*), and especially accessory basal (AB) nuclei (*B*). In the macaque, MET staining is also enriched in the L and B nuclei (*D* and *E*) as compared with the (AB) and amygdalohippocampal (AHA) nuclei (*E* and *F*), indicating that Met/MET is differentially expressed by select amygdaloid afferents during development. The boxed region in schematized macaque brain sections corresponds to the photomicrograph directly above. The posteroanterior (P← →A) position of macaque sections is indicated in schematized, dorsal views of the brain. AAA, anterior amygdaloid area; Ce, central amygdaloid nucleus; ec, external capsule; S, subiculum; ST. Scale bar = 275 μM for (A–C); 770 μM for (*D–F*).

efferent amygdala axons also course within the external capsule and the anterior commissure, both of which are clearly labeled in the mouse (Figs. 2*A,B* and 6*A*; Fig. 10*A–C*) and macaque (Figs 2*D,E* and 10*G,H*) forebrain at corresponding developmental stages.

Patterns of Met/MET expression within the mouse and macaque hippocampus were generally conserved. The molecular layer of the dentate gyrus and cornu ammonis (CA) fields of the hippocampus, throughout the anteroposterior extent, contained Met/MET immunoreactivity in both the P7 mouse (Fig. 5*A–C*) and GD150 macaque (Fig. 5*D–F*), consistent with Met/MET expression in perforant pathway axon projections from entorhinal cortex in both species. However, the intensity of Met/MET staining in the molecular layer was relatively stronger in the mouse as compared with the macaque. Densely stained neuropil at the subiculum/CA1 boundary constituted a hippocampal MET-labeling feature specific to the macaque, which was most salient in posterior sections (Fig. 5*D–F*).

Met/MET labeling was intense at P7 in the mouse and GD150 in the monkey in the axon tracts that contain and the target regions that receive hippocampal efferent axon projections. For example, immunostaining was observed in the precommissural fornix (Fig. 6*A,C,E*). One of the most robust projections of the subiculum via the postcommissural fornix is to the medial mammillary nucleus. Met/MET neuropil labeling was dense in the medial mammillary nucleus in both the P7 mouse (Fig. 6*B*) and the GD150 macaque (Fig. 6*D,F*), consistent with high expression levels of the receptor in terminal axons of this subicular efferent pathway. However, a subset of axon fascicles in the indusium griseum (IG), a structure considered to be an extension of the hippocampus (Wyss and Sripanidkulchai 1983), was densely labeled in the macaque (Supplementary Fig. 3J) but not the mouse (Supplementary Fig. 3G–I). The staining was much less intense at GD150 than GD100 and was undetectable by P21 (Supplementary Fig. 3J–L). As shown in coronal sections that include the postcommissural fornix, a similar temporal dynamic of MET expression was observed in hippocampal efferent axons in the macaque (Fig. 7*D–F*), a pattern that also was evident in the mouse (Fig. 7*A–C*). Collectively, these data demonstrate that Met/MET is expressed transiently at high levels in afferent and efferent axons of the amygdala and hippocampal formation during early periods of circuit wiring in the mouse and macaque forebrain, followed by a significant reduction to much lower levels later postnatally.

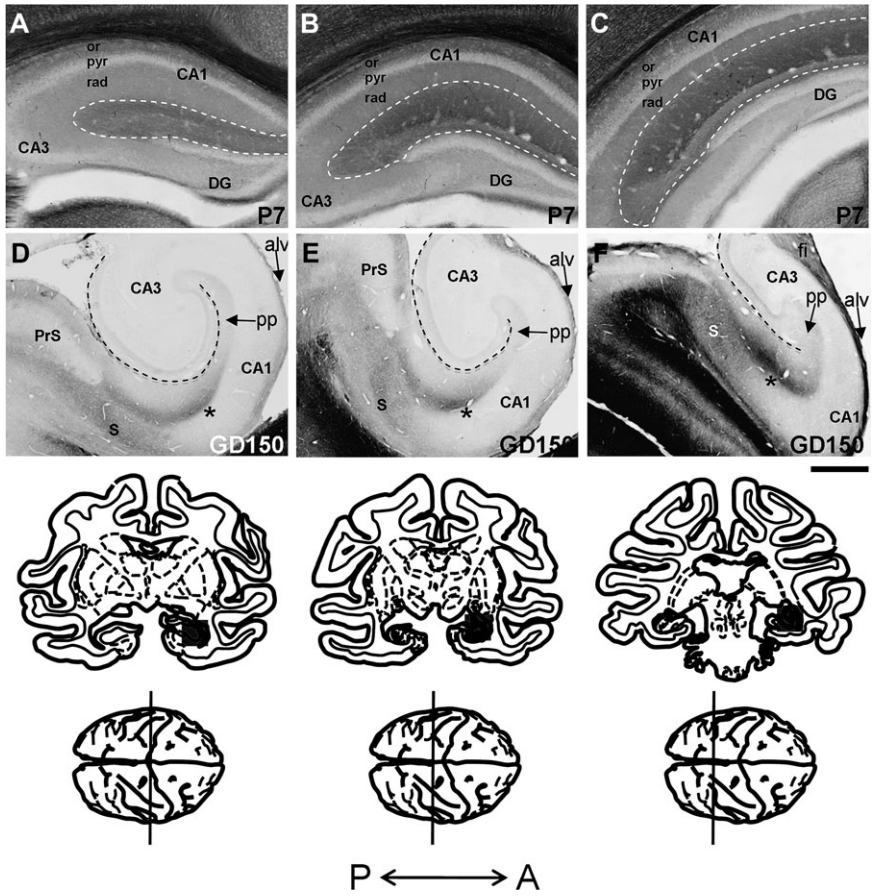

Figure 5. Conserved Met/Met expression in hippocampal afferents. Differential interference contrast photomicrographs illustrate Met/MET immunohistochemistry at various anteroposterior levels of the hippocampus in coronal brain sections from the P7 mouse and GD150 macaque. In both the developing mouse (*A–C*) and macaque (*D–F*), Met/MET staining is observed in entorhinal cortical projections of the perforant pathway (pp) within the molecular layer. The perforated boundary in mouse panels encompasses the molecular layer of both the dentate gyrus (DG) and cornu ammonis (CA) subfields but bounds only that of the DG in macaque panels. Additional more intense MET labeling is focused in the region overlaying the stratum radiatum (rad) at the subiculum/CA1 boundary (asterisks in *D*, *E*, and *F*). Staining patterns in both species are most salient at posterior (mouse *B* and *C*; macaque *E* and *F*) as opposed to anterior (mouse *A*; macaque *D*) levels. The boxed region in schematized macaque brain sections corresponds to the photomicrograph directly above. The posteroanterior (P← →A) position of macaque sections is indicated in schematized dorsal views of the brain. alv, alveus; CA1, cornu ammonis 1 of hippocampus; CA3, cornu ammonis 3 of hippocampus; fi, fimbria; or, stratum oriens; PrS, presubiculum; pyr, pyramidal cell layer; S, subiculum. Scale bar = 275 μM for (*A–C*); 770 μM for (*D–F*).

Comparative Analysis of Tangential Patterns of Neocortical Met/MET Expression

Mice and primates depend differentially on specific sensory modalities for communicating with conspecifics. Thus, we extended our analysis to interspecies comparisons of Met/MET expression within sensory and associative neocortical areas during forebrain circuit development. As shown in low-magnification images representing the anteroposterior extent of the P0 mouse forebrain (Fig. 8*A–D*), Met immunohistochemical staining was broadly distributed across the tangential domain of the mouse neocortex, with particularly robust labeling throughout the major tracts carrying corticocortical and corticofugal axon projections, including the corpus callosum, anterior commissure, and internal capsule. This broad tangential distribution of neocortical Met expression was more readily apparent in a similar anteroposterior array of Met-stained sections at P7 (Fig. 9*A–D*), when neuropil expression of the receptor proved to be at its peak. Moreover, the patterns of staining within major subcortical corticofugal axon terminal fields reflected the widespread Met expression in the neocortical neuropil and axon tracts containing corticofugal efferents (e.g., the internal capsule). As shown at P7, Met-labeled neuropil was evident both throughout the striatum (Fig. 10*A–C*) and within many nuclei of the thalamus (Fig. 10*D–F*).

In contrast, there was a remarkably restricted pattern of MET expression in the macaque neocortex at GD100 and GD150. MET labeling was largely absent in the frontal lobes, except for low neuropil expression in medial areas that included the anterior cingulate and subgenual cortices (Figs 8*A* and 9*A*). While still modest in staining intensity, there was a progressive increase in the intensity of MET labeling at increasingly posterior levels of the cingulate cortex (areas 24 and 23). This pattern was marked most saliently by staining in the cingulum at GD100 and in the cortical neuropil at GD150 (Figs 8*A–D* and 9*A–D*). The most robust staining for MET at GD100 was evident in the subplate and neocortical white matter underlying extrastriate visual and auditory cortices of the temporal, inferior parietal, and occipital lobes across anteroposterior levels of the macaque forebrain (Fig. 8*B–D*). By GD150, expression had expanded to include the neuropil within these selective neocortical regions (Fig. 9*B–D*). Neuropil staining patterns at GD150 were also highly complex within these regions, especially in the temporal lobe. Labeling was most intense inferior to the superior temporal sulcus. This region

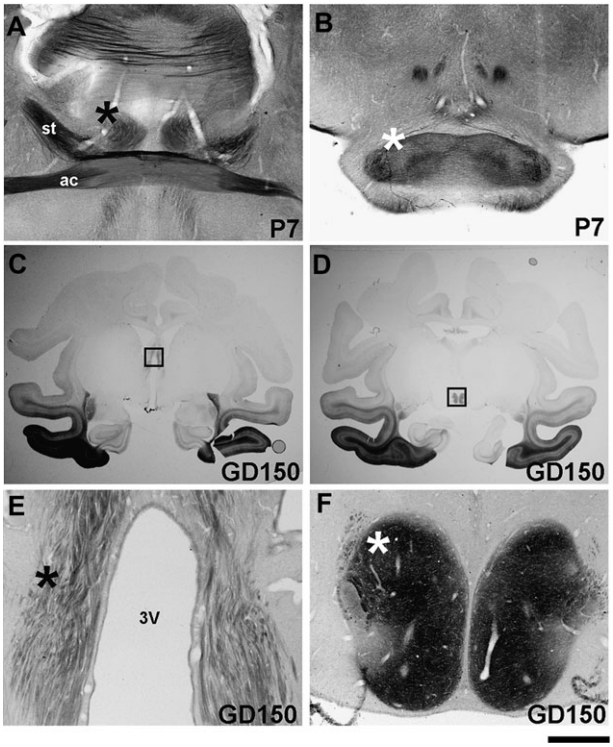

Figure 6. Conserved Met/MET expression in efferents of the hippocampal formation. Photomicrographs illustrate Met/MET immunohistochemistry in fiber tracts and axon terminal fields in coronal forebrain sections from the P7 mouse and GD150 macaque. (*A* and *B*): Examples of Met staining in the precommissural fornix (black asterisk) and mammillary bodies (white asterisk) in the developing mouse forebrain. Corresponding MET-stained structures are observed in the macaque during a similar developmental period as shown at low- (*C* and *D*) as well as high-magnification (*E*, boxed region in *C*, black asterisk; *F*, boxed region in *D*, white asterisk). ac, anterior commissure; 3V, third ventricle; LV, lateral ventricle; ST. Scale bar = 550 μM for (*A*), (*B*) and (*E*), (*F*); 9.48 mm for (*C*) and (*D*).

contains high-order unimodal visual areas, with neurons that are responsive to complex stimuli including scenes, objects, and primate faces (Baylis et al. 1987; Tsao et al. 2006) (Fig. 9*B–D*). Much less intense MET staining was present superior to the STS in polysensory and associative auditory cortices within the superior temporal gyri (Fig. 9*B–D*) and inferior parietal lobes (Fig. 9*C,D*).

The limited tangential extent of MET expression in the developing macaque neocortex was highly divergent from the mouse and was reflected in the restricted subsets of forebrain axon tracts and presumed cortical efferent axon target areas that were MET stained. Dense MET labeling in the anterior commissure was evident, consistent with receptor expression in crossing corticocortically projecting neurons within the temporal lobes (Figs 8*B* and 9*B*). MET staining also was present in the external and extreme capsules within the ventral forebrain, which presumably distribute MET-expressing axons ipsilaterally among interconnected temporal cortices and to highly specific regions of the striatum (Figs 8*A*, 9*A*, and 10*G,H*). A small minority of efferent amygdala axons could also contribute to the staining in this tract. Ventral striatal areas, including the olfactory tubercle, ventral putamen, and tail of the caudate nucleus constituted the most notable target areas of presumed MET-labeled terminal axons in the macaque (Fig. 10*G,H*). There also was very light staining in the nucleus accumbens (Fig. 10*G*). All other striatal areas were consistently devoid of MET staining (Fig. 10*G–I*), save for the dorsal caudate nucleus in which light and very spatially limited labeling was observed (Fig. 10*G,I*).

MET was expressed in a limited subgroup of presumed corticothalamic efferent axons, consistent again with the highly restricted staining in the neocortex. For example, moderate neuropil staining in the laterodorsal superficial (data not shown) and anteroventral (Fig. 10*I*) thalamic nuclei are consistent with the observation of MET expression in the cingulate cortices. The most robust MET staining in the dorsal thalamus was found in subnuclei of the pulvinar. Specifically, the staining was concentrated in the inferior and lateral subdivisions of the pulvinar, with much reduced labeling in the medial subdivsion (Fig. 10*J*). This pattern reflects the foci of MET expression in the temporal and inferior parietal lobes. Finally, like in mouse, the posterior reticular nucleus contained MET-labeled neuropil in the monkey (Fig. 10*J*). All other thalamic nuclei in the developing macaque were devoid of MET staining.

Discussion

The present data provide a descriptive developmental analysis of the receptor proteins encoded by orthologs of the ASD risk gene, *MET*, yielding new insight regarding the most vulnerable circuits in the developing primate brain that would not be evident from mouse expression analyses alone. A summary of our comparative findings is included in Table 1. The conserved temporal and subcortical patterns of expression for mouse Met and the macaque homologue, MET, suggest a role for the receptor in forebrain circuit wiring. We found that in both species, prior to the plateau phase of peak synaptogenesis, Met/MET receptor expression expanded within growing axons and in cortical and subcortical neuropil, coinciding with the robust collateralization of these axons within their terminal fields. These patterns suggest a presynaptically derived role for Met/MET signaling in the initial wiring of the cortex with forebrain centers that process socially and emotionally relevant information. Consistent with this, we have found that the ablation of Met signaling selectively from the neocortex in the mouse alters dendrite and dendritic spine morphology in cortical and subcortical target neurons (Judson et al. 2010).

Despite the remarkable similarity in subcellular receptor distributions discussed above, it should be noted that our Met/MET immunohistochemical stain provides inadequate resolution either to distinguish the staining of axonal versus dendritic elements or to differentiate between multiple sources of axonal afferents, within the neuropil. We previously circumvented this issue in the mouse by additionally analyzing wild-type patterns of *Met* transcript expression as well as Met staining patterns in a dorsal pallium-specific conditional Met knockout mouse. This approach allowed us to determine that nearly all Met staining in the subcortical neuropil is localized to axonal afferents of a dorsal pallial origin. In order to determine the extent to which this finding applies to similar MET staining patterns in the macaque forebrain, we would ultimately need to analyze developmental *MET* transcript expression. There is, however, considerable indirect evidence supporting the preferential localization of MET to dorsally derived axonal compartments in the subcortical neuropil. For example, the ventral (high) to dorsal (low) gradient of MET staining in the temporal cortex is reflected with remarkable fidelity in the ventrolateral (high) to

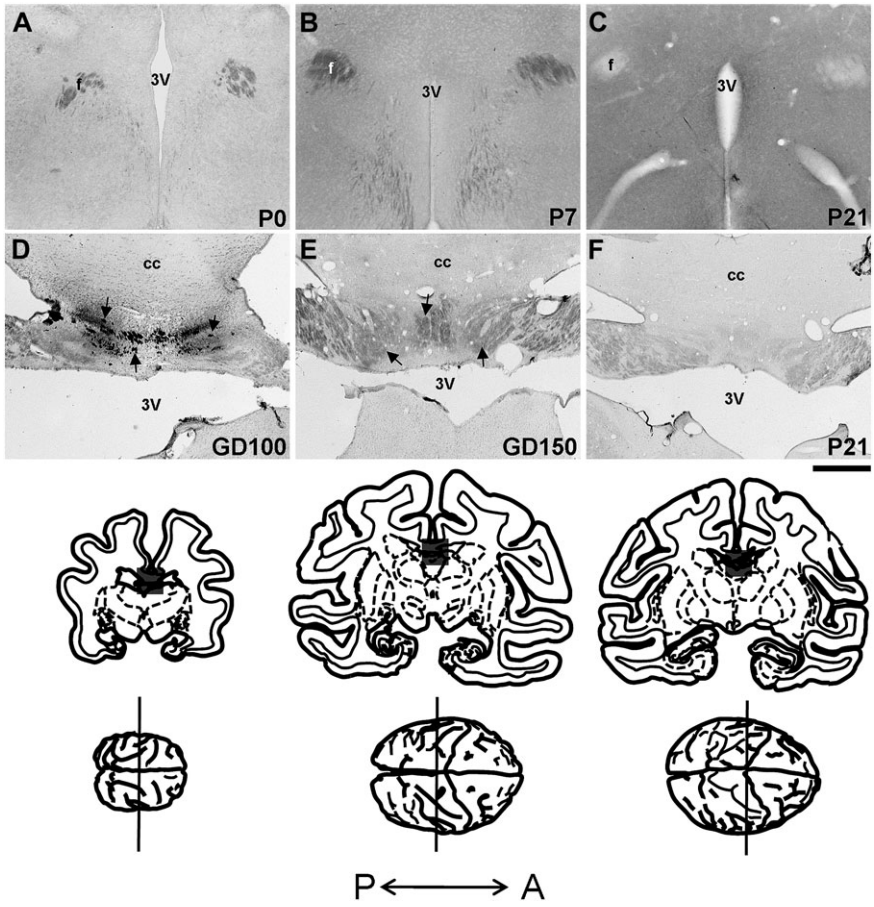

Figure 7. Conserved temporal patterns of Met/MET expression in the fornix. Differential interference contrast photomicrographs illustrate Met/MET immunohistochemistry in mouse and macaque coronal brain sections during development. Met/MET staining in efferent fibers of the hippocampus decreases developmentally in the mouse (*A–C*) and macaque (*D–F*). Axons of the postcommissural fornix (f) are shown in cross-section in mouse panels (*A–C*). The macaque f, inferior to the corpus callosum (cc), is depicted in (*D–F*). Examples of select intensely stained axon bundles are indicated by arrows (*D* and *E*). The boxed region in schematized macaque brain sections corresponds to the photomicrograph directly above. The posteroanterior (P ⟵ ⟶ A) position of macaque sections is indicated in schematized dorsal views of the brain. 3V, third ventricle. Scale bar = 275 μM for (*A–C*); 1.1 mm for (*D–F*).

dorsomedial (low) gradient of staining in the pulvinar, consistent with the topographical organization of temporal corticothalamic axon projections within this nucleus (Romanski et al. 1997; Yeterian and Pandya 1997; Shipp 2003)

Divergent Patterns of Met/MET Expression are Consistent with Species-Specific Modes of Social Communication

This study has revealed 2 themes concerning spatial patterns of Met/MET expression: 1) in both species, receptor expression is conserved within limbic structures that are essential for social cognition and memory, including the hippocampus, amygdala, and cingulate cortices and 2) patterns of receptor expression diverge within sensory and associative neocortical areas according to species-specific specializations in sensory perception. Evidence supporting the first theme comes from the observation of shared Met/MET expression in the structures and axon pathways that constitute core limbic circuitry (Papez 1937; MacLean 1955). Significant developmental Met/MET expression was observed in hippocampal efferent axons projecting to the medial mammillary bodies, in axon terminals within the anteroventral thalamic nucleus, in the neuropil of the cingulate cortex, in axons within the cingulum, and in the hippocampal complex, effectively completing the classically defined circuit of Papez (Papez 1937). Met/MET expression also was shared in the main efferent pathway of the amygdala, the ST, and, though less obvious in the macaque, medial and orbital prefrontal cortical areas, indicating conserved receptor function in the development of broader, more modernly defined limbic circuits (MacLean 1955; Nauta 1971; Barbas 2000; Ongur and Price 2000). This evolutionary conservation of Met/MET expression is not surprising; the limbic brain is phylogenetically old, and conserved expression of other molecules that participate in limbic circuit wiring has been reported (Horton and Levitt 1988; Chesselet et al. 1991; Pimenta et al. 1996). There are, however, emergent differences that we noted. For example, MET expression in the IG appeared to be a unique feature of the developing primate limbic system, and Met-labeled afferents within the olfactory amygdala were detected only in mouse. Additionally, MET staining in the ventromedial striatum may be localized in part to afferents originating in the basolateral amygdala and/or hippocampal formation (Friedman et al. 2002), a pattern not detected in the mouse (Judson et al. 2009). However, as demonstrated in the present study, the greatest interspecies divergence in patterns of Met/MET expression during social circuit development is at the level of the neocortex.

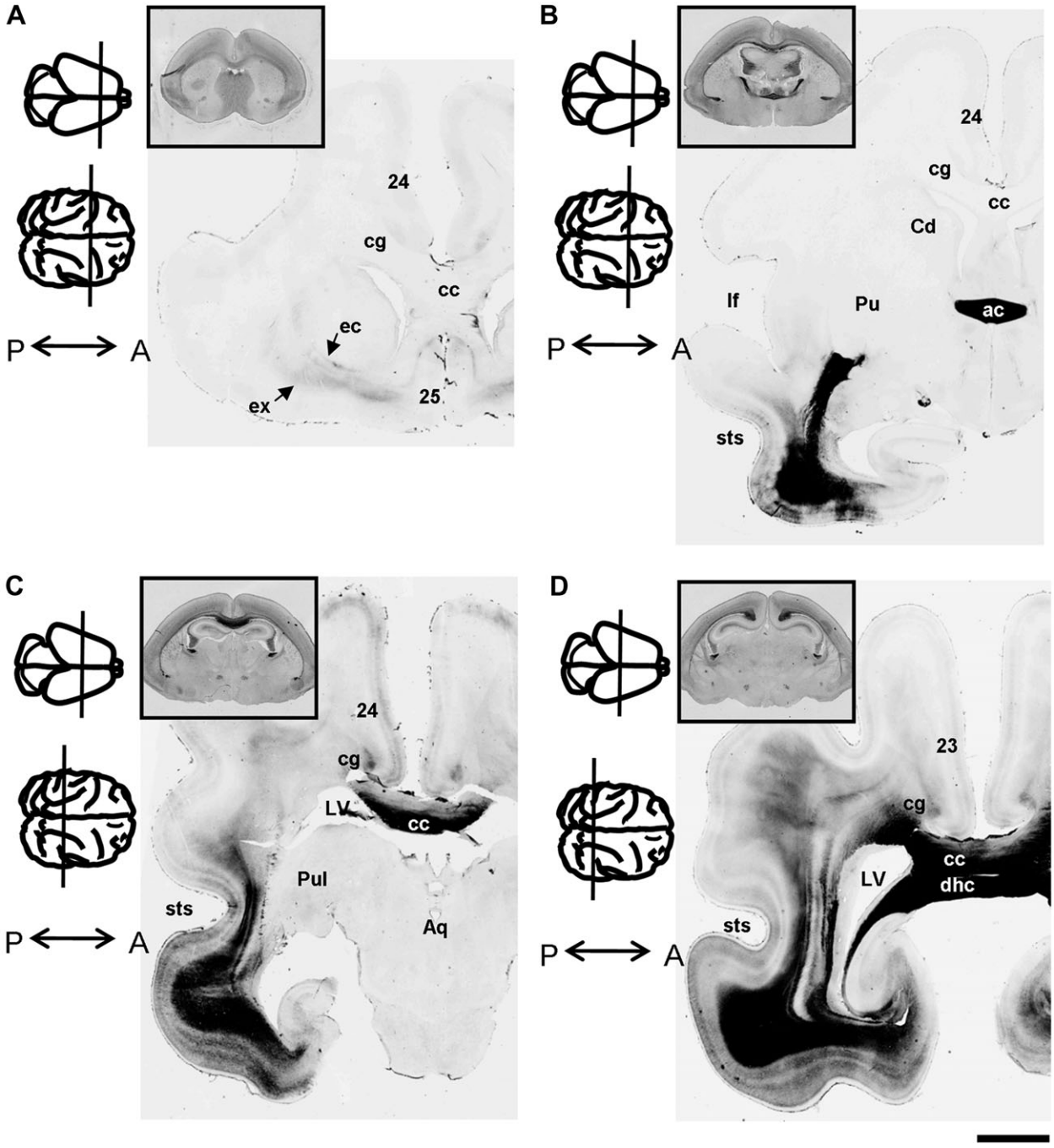

Figure 8. Divergent spatial patterns of neocortical Met/MET expression in the developing mouse and macaque forebrain. Differential interference contrast photomicrographs illustrate the anterior (*A*) to posterior (*D*) progression of Met/MET immunohistochemistry in coronal forebrain sections from the P0 mouse and GD100 macaque. Notably, all major fiber tracts that carry corticofugal projections as well as the subplate exhibit intense Met staining in the mouse forebrain (inset images, *A–D*). Robust MET expression in the macaque is largely confined to the subplate underlying cortices inferior to the superior temporal sulcus (sts) and in select corticofugal fiber tracts of the incipient temporal lobe including, most notably, the anterior commissure (ac, *B*) as well as the external (ec) and extreme (ex) capusules anteriorly (*A*). Additional staining in the cingulum (cg, *A–D*) likely reflects MET expression in the efferent fibers of the posterior cingulate cortex, whereas labeled axons of the corpus callosum (cc, *A–D*) may originate in the posterior cingulate and/or cortices inferior to the intraparietal sulcus (ips). The posteroanterior (P← →A) level of mouse (top) and macaque (bottom) sections is indicated in schematized dorsal views of the brain to the left of each figure panel. 24, cortical area 24; 25, cortical area 25; Aq, cerebral aquaduct; Cd, caudate; dhc, dorsal hippocampal commissure; lf, lateral fissure; LV, lateral ventricle; Pu, putamen; Pul, pulvinar. Scale bar = 3.15 mm for all macaque images; 2.3 mm for inset mouse images.

The conserved presence of MET-expressing cortical afferents within the basolateral amygdala, cingulate cortex, perirhinal cortex, and entorhinal cortex evokes some speculation about the relevance to social information processing. This feature suggests a role for the receptor in developing an interface between cortical circuits required for social perception and downstream limbic circuits that facilitate social cognitive processes such as social recognition, arousal, and awareness (Adolphs 2001; Amaral 2003; Phelps and LeDoux 2005). Because the neocortical expression patterns overlap functional areas required for the receipt of socially relevant stimuli characteristic of each species,

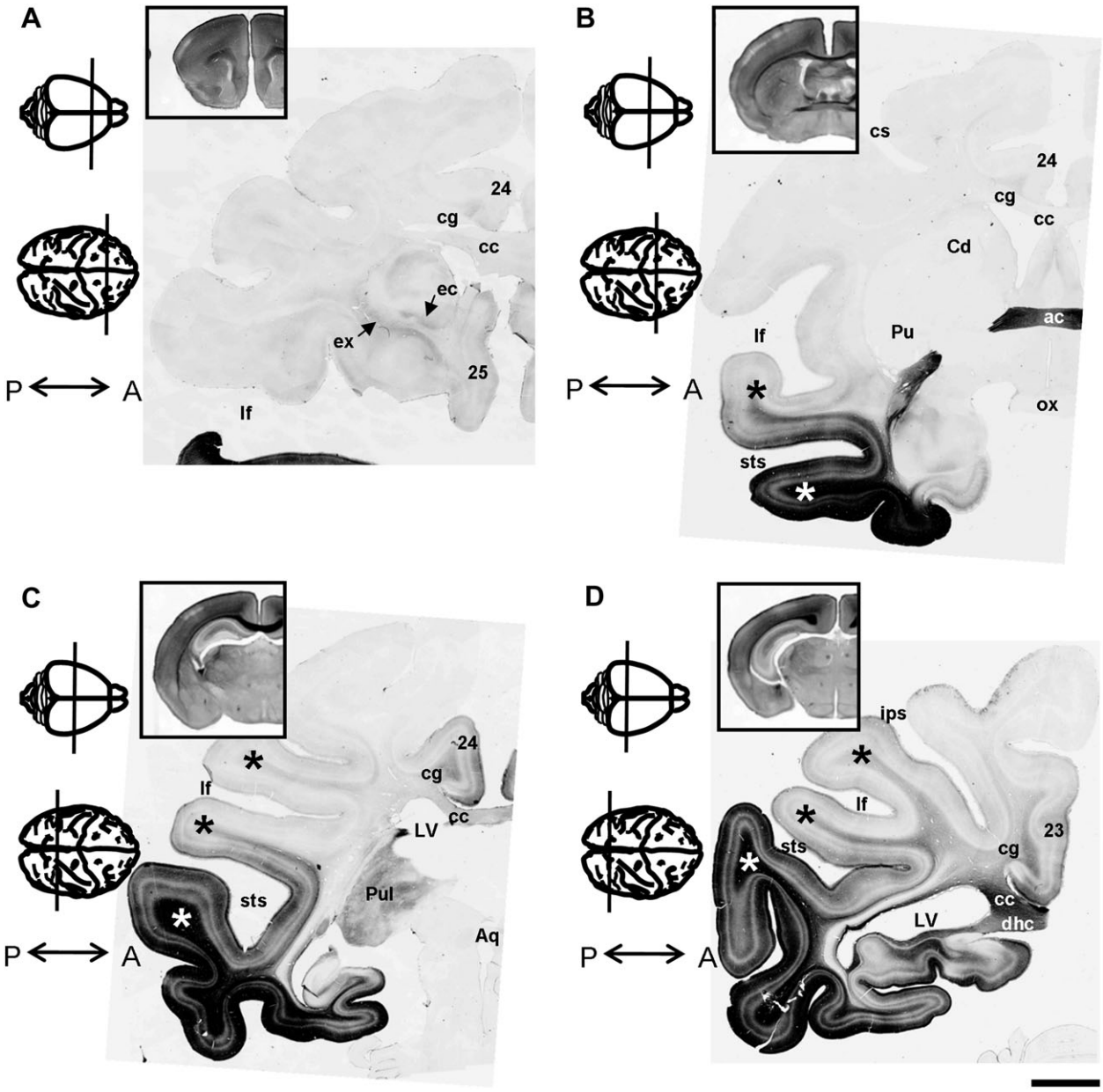

Figure 9. Divergent spatial patterns of neocortical Met/MET expression in the developing mouse and macaque forebrain. Differential interference contrast photomicrographs illustrate the anterior (*A*) to posterior (*D*) progression of Met/MET immunohistochemistry in coronal forebrain sections from the P7 mouse and GD150 macaque. While Met expression in the mouse (inset images, *A–D*) is broadly distributed throughout the tangential domain of the neocortex, MET expression in the macaque is largely restricted to the temporal cortices (white and black asterisks, *B–D*) and midline cortices including the anterior cingulate cortex (cortical area 24, *A–C*; area 23, *D*) and subgenual cortex (area 25, *A*). MET is also differentially expressed within the macaque temporal lobe; staining is strong inferior to (white asterisks, *B–D*), and of modest intensity superior to (black asterisks, *B–D*), the superior temporal sulcus (sts). Axon staining within the cingulum (cg, *A–D*), anterior commissure (ac, *B*), and posterior regions of the corpus callosum (cc, *C* and *D*) reflect the restricted populations of neocorticocortical projection neurons that express MET. The posteroanterior (P← →A) level of mouse (top) and macaque (bottom) sections is indicated in schematized dorsal views of the brain to the left of each figure panel. Aq, cerebral aquaduct; Cd, caudate; cs, central sulcus; dhc, dorsal hippocampal commissure; ec, external capsule; ex, extreme capsule; ips, intraparietal sulcus; lf, lateral fissure; LV, lateral ventricle; ox, optic chiasm; Pu, putamen; Pul, pulvinar. Scale bar = 4.6 mm for all macaque images; 2.8 mm for inset mouse images.

we hypothesize that Met/MET signaling may have been evolutionarily co-opted to participate in the integration of circuits involved in the perception of socially and emotionally relevant information. This will need to be tested directly through manipulation of gene expression and behavioral testing.

In primate species such as the macaque, sensory faculties such as vision and audition are critical to the perception of socially relevant stimuli, and they are largely rooted in neocortical areas of the temporal, occipital, and inferior parietal lobes. Remarkably, during the wiring of circuits in these regions, we observed a nearly exclusive localization of MET to the axons of projection neurons. MET expression was particularly dense in the inferior temporal gyrus, which contains unimodal cortical areas in the ventral visual stream that process the features of complex socially relevant visual stimuli including body parts and faces (Pinsk et al. 2005; Tsao and Livingstone 2008; Pinsk et al. 2009). Because we also

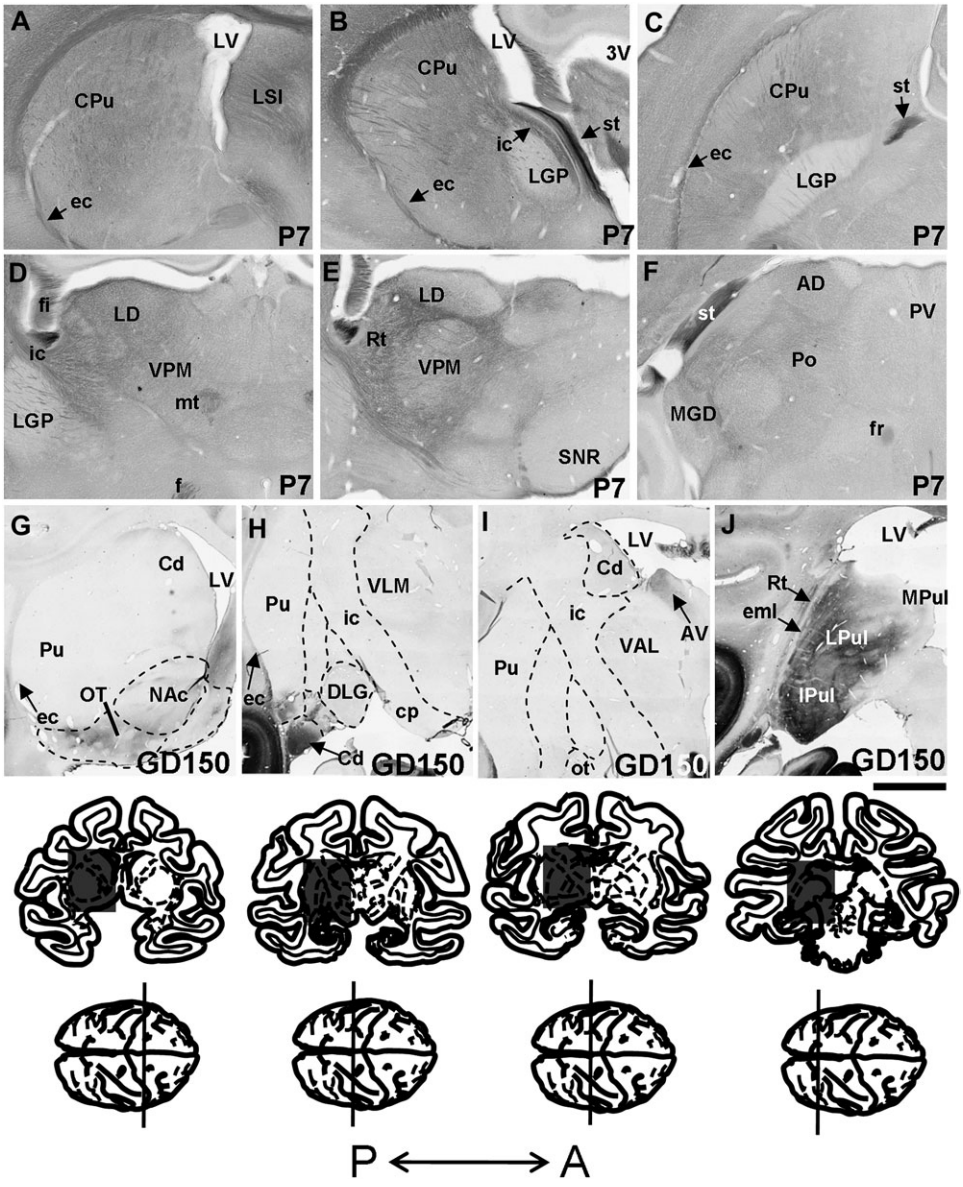

Figure 10. Met/MET expression in neocortical efferents in the developing mouse and macaque forebrain. Differential interference contrast photomicrographs illustrate Met/MET immunohistochemistry in forebrain sections from the P7 mouse and GD150 macaque. Widespread Met labeling is observed in the neuropil of the caudatoputamen (CPu) (*A*, *B*, and *C*) and lateral thalamus (*D*, *E*, and *F*) in coronal (*A* and *D*), sagittal (*B* and *E*), and horizontal (*C* and *F*) brain sections of the developing mouse forebrain, consistent with widespread Met expression in long-projecting axons of the neocortex. The distribution of MET-labeled neocortical efferents in the developing macaque striatum is much more restricted as robust staining is observed only in the olfactory tubercle (OT) (*G*) and the ventral putamen (Pu) and caudate (Cd) (*H*). Areas of lighter striatal MET staining include the nucleus accumbens (NAc) (*G*) and restricted regions within the dorsal Cd (*G* and *I*). MET-labeled neocortical efferents to the macaque thalamus are predominantly restricted to the reticular nucleus (Rt) (*J*), lateral (LPul) and inferior (IPul) pulvinar nuclei (*J*), and limbic thalamic nuclei including the anteroventral nucleus (AV) (*I*). The boxed region in schematized macaque brain sections corresponds to the photomicrograph directly above. The posteroanterior (P← →A) position of macaque sections is indicated in schematized dorsal views of the brain. 3V, third ventricle; AD, anterodorsal thalamic nucleus; cp, cerebral peduncle; DLG, dorsolateral geniculate nucleus; ec, external capsule; eml, external medullary lamina; f, fornix; fi, fimbria of hippocampus; fr, fasciculus retroflexus; ic, internal capsule; LD, laterodorsal thalamic nucleus; LGP, lateral globus palidus; LV; lateral ventricle; LSI, intermediate lateral septal nucleus; MGD, medial geniculate nucleus, dorsal part; MPul, medial pulvinar nucleus; mt, mammillothalamic tract; Po, posterior thalamic nuclear group; PV, paraventricular thalamic nucleus; SNR, substantia nigra pars reticulata; ST; VAL, ventral anterior thalamic nucleus, lateral part; VLM, ventrolateral thalamic nucleus, medial part; VPM, ventral posteromedial thalamic nucleus. Scale bar = 550 μM for (*A*–*F*); 3.39 mm for (*G*–*J*).

observed MET staining of presumed inferotemporal cortical efferent axons within the perirhinal and entorhinal cortices of the hippocampal complex, we suggest that the receptor may influence the development of circuits required for social recognition (Malkova et al. 1995; Thornton et al. 1997)—an essential cognitive process supporting social interaction among primate conspecifics. Additionally, staining was observed in the ventral putamen and caudate nucleus of the striatum, indicating that the development of circuits governing the formation of socially adaptive visual habits also may depend in part on intact MET signaling (Fernandez-Ruiz et al. 2001).

Whereas neocortical MET expression was spatially restricted in the tangential domain, perhaps reflecting the dependence of primates on auditory and especially visual sensation for social interaction, Met expression in the mouse neocortex was broadly distributed. Considering the current understanding that rodent species depend heavily on somatosensation and olfaction

Table 1
Summary of comparative forebrain Met/MET expression

Brain region or tract	Mouse Met expression			Macaque MET expression		
	P0	P7	P21	GD100	GD150	P21
Prefrontal cortex, lateral	L	H	L	nd	nd	nd
Prefrontal cortex, medial	L	H	L	nd	L	nd
Anterior cingulate cortex, anterior	L	M	L	L	M	L
Anterior cingulate cortex, posterior	L	M	L	M	H	L
Frontal cortex, motor	L	H	L	nd	nd	nd
Parietal cortex, somatosensory	L	H	L	nd	nd	nd
Parietal cortex, association	M	H	L	L	M	L
Temporal cortex, auditory	M	H	L	L	M	L
Temporal cortex, visual	na	na	na	M	H	L
Temporal cortex, association	M	H	L	L	M	L
Occipital cortex	M	H	L	M	H	L
Perirhinal cortex	M	H	L	M	H	L
Entorhinal cortex	M	H	L	L	M	L
Hippocampus, subiculum	M	H	L	L	M	nd
Hippocampus, CA1	M	H	L	L	M	nd
Hippocampus, CA3	L	M	L	nd	nd	nd
Hippocampus, DG	nd	nd	nd	nd	nd	nd
Hippocampus, molecular layer	L	M	L	L	M	L
IG	nd	nd	nd	H	L	nd
Amygdala, NLOT	M	H	L	nd	nd	nd
Amygdala, medial	L	M	L	nd	nd	nd
Amygdala, lateral	L	H	L	L	M	nd
Amygdala, basal	L	M	L	L	M	nd
Amygdala, accessory basal	L	M	L	nd	L	nd
Amygdala, posterior cortical	M	H	L	nd	nd	nd
Striatum, caudate/putamen	L	H	L	L, ventral	H, ventral	L, ventral
Striatum, globus pallidus	nd	nd	nd	nd	nd	nd
Striatum, olfactory tubercle	L	M	nd	L	M	L
Striatum, nucleus accumbens	nd	nd	nd	nd	L	nd
Thalamus, reticular nucleus	L	M	nd	nd	M	nd
Thalamus, anteroventral	nd	M	L	nd	M	nd
Thalamus, ventrolateral	L	M	L	nd	nd	nd
Thalamus, medial pulvinar	na	na	na	nd	L	nd
Thalamus, lateral pulvinar	na	na	na	nd	M	nd
Thalamus, inferior pulvinar	na	na	na	L	H	L
Hypothalamus, medial mammillary nuclei	L	H	L	L	H	L
Hypothalamus, lateral mammillary nuclei	nd	nd	nd	nd	nd	nd
Corpus callosum, anterior	L	M	L	nd	nd	nd
Corpus callosum, intermediate	M	H	L	M	L	nd
Corpus, callosum, posterior	H	H	L	H	M	L
Cingulum, anterior	M	L	L	L	L	nd
Cingulum, posterior	M	L	L	H	M	L
Anterior commissure, body	M	L	L	H	M	L
Internal capsule	M	L	L	nd	nd	nd
External capsule	H	M	L	L	L	nd
Extreme capsule	L	L	nd	L	L	nd
Precommissural fornix	H	M	L	H	M	L
Postcommissural fornix	H	M	L	H	M	L
Dorsal hippocampal commissure	H	M	L	H	M	L
ST, subset of fibers	H	M	L	H	M	L

Note: L, light labeling; M, moderate labeling; H, heavy labeling; nd, not detected; na, not applicable.

(Brennan and Kendrick 2006; Spehr et al. 2006) in order to communicate, this pattern could be considered nonspecific with regard to social sensory specialization in the mouse. Two recent findings, however, demonstrate that mice are also quite adept at using vision and audition to extract socially relevant information from their environment. First, Langford et al. (2006) demonstrated that the visual observation of pain-related behavior in a conspecific subject can modulate pain responses in an observer mouse through an empathy-like process. Second, exposure to conspecific vocalizations was shown to modulate fear conditioning in mice, also through an empathy-like process (Chen et al. 2009). Finally, tail rattling, an important behavioral trait associated with mouse aggression (St John 1973), is also perceived by the auditory and/or visual senses.

MET Expression Patterns and Circuit Vulnerability in Autism

Recent studies from multiple laboratories have established human *MET* gene promoter variants as causative risk alleles for ASD. The *MET* rs1858830-C allele in particular has been shown to promote less efficient MET transcription in in vitro assays [Campbell et al. 2006]), consistent with the clinical observation of a 2-fold reduction of MET expression in the temporal cortex of postmortem tissue harvested from subjects with ASD (Campbell et al. 2007). However, we believe that data from the present study indicate that alterations in the spatial and temporal distributions of MET expression may be as important to consider as the absolute levels of expression with regard to the wiring of circuits in the primate brain. Though more limited in scope, our initial mapping of MET expression in the developing human forebrain is consistent with the macaque studies presented here (Mukamel Z, Konopka G, Wexler E, Dong H, Osborn G, Bergman M, Levitt P, Geschwind D, unpublished data). Moreover, considering the population frequencies (0.35–0.55) of ASD-associated *MET* alleles (Campbell et al. 2006; Campbell et al. 2008; Jackson et al. 2009; Sousa et al. 2009), mapping studies of brains with *MET* risk allele genotypes may help to elucidate broadly relevant etiological mechanisms of the disorder.

Supplementary Material

Supplementary material can be found at: http://www.cercor.oxfordjournals.org/.

Funding

National Institutes of Health (NIH)/National Institute of Mental Health (NIMH) (MH067842 to P.L.); NIH/National Institute of Child Health and Human Development (P30 HD15052 to E. Dykens); NIH/National Institute on Drug Abuse (DA022785 to P.L.); Simons Foundation to P.L.; NIH/NIMH (MH41479 to D.G.A.); NARSAD to D.G.A. and was conducted, in part, at the California National Primate Research Center (P51 RR0000169).

Notes

We thank Dr Larry Swanson for his helpful insights and discussions, which facilitated the preparation of this manuscript. We also thank Deborah Gregory, Donte Smith, and Kate Spencer in the Levitt laboratory for excellent assistance in maintaining the mouse colony and Jeff Bennett in the Amaral laboratory for preparing the macaque brain sections used in this study. *Conflict of Interest* : None declared.

References

Adolphs R. 2001. The neurobiology of social cognition. Curr Opin Neurobiol. 11:231–239.

Amaral DG. 2003. The amygdala, social behavior, and danger detection. Ann N Y Acad Sci. 1000:337–347.

Barbas H. 2000. Connections underlying the synthesis of cognition, memory, and emotion in primate prefrontal cortices. Brain Res Bull. 52:319–330.

Baylis GC, Rolls ET, Leonard CM. 1987. Functional subdivisions of the temporal lobe neocortex. J Neurosci. 7:330–342.

Bourgeois JP, Goldman-Rakic PS, Rakic P. 1994. Synaptogenesis in the prefrontal cortex of rhesus monkeys. Cereb Cortex. 4:78–96.

Bourgeois JP, Rakic P. 1993. Changes of synaptic density in the primary visual cortex of the macaque monkey from fetal to adult stage. J Neurosci. 13:2801–2820.

Brennan PA, Kendrick KM. 2006. Mammalian social odours: attraction and individual recognition. Philos Trans R Soc Lond B Biol Sci. 361:2061–2078.
Campbell DB, D'Oronzio R, Garbett K, Ebert PJ, Mirnics K, Levitt P, Persico AM. 2007. Disruption of cerebral cortex MET signaling in autism spectrum disorder. Ann Neurol. 62:243–250.
Campbell DB, Li C, Sutcliffe JS, Persico AM, Levitt P. 2008. Genetic evidence implicating multiple genes in the MET receptor tyrosine kinase pathway in autism spectrum disorder. Autism Res. 1:159–168.
Campbell DB, Sutcliffe JS, Ebert PJ, Militerni R, Bravaccio C, Trillo S, Elia M, Schneider C, Melmed R, Sacco R, et al. 2006. A genetic variant that disrupts MET transcription is associated with autism. Proc Natl Acad Sci U S A. 103:16834–16839.
Campbell DB, Warren D, Sutcliffe JS, Lee EB, Levitt P. 2010. Association of MET with social and communication phenotypes in individuals with autism spectrum disorder. Am J Med Genet B Neuropsychiatr Genet. 153B:438–446.
Chen Q, Panksepp JB, Lahvis GP. 2009. Empathy is moderated by genetic background in mice. PLoS One. 4:e4387.
Chesselet MF, Gonzales C, Levitt P. 1991. Heterogeneous distribution of the limbic system-associated membrane protein in the caudate nucleus and substantia nigra of the cat. Neuroscience. 40:725–733.
Ebens A, Brose K, Leonardo ED, Hanson MG, Jr., Bladt F, Birchmeier C, Barres BA, Tessier-Lavigne M. 1996. Hepatocyte growth factor/scatter factor is an axonal chemoattractant and a neurotrophic factor for spinal motor neurons. Neuron. 17:1157–1172.
Fernandez-Ruiz J, Wang J, Aigner TG, Mishkin M. 2001. Visual habit formation in monkeys with neurotoxic lesions of the ventrocaudal neostriatum. Proc Natl Acad Sci U S A. 98:4196–4201.
Friedman DP, Aggleton JP, Saunders RC. 2002. Comparison of hippocampal, amygdala, and perirhinal projections to the nucleus accumbens: combined anterograde and retrograde tracing study in the Macaque brain. J Comp Neurol. 450:345–365.
Frith C. 2004. Is autism a disconnection disorder? Lancet Neurol. 3:577.
Geschwind DH, Levitt P. 2007. Autism spectrum disorders: developmental disconnection syndromes. Curr Opin Neurobiol. 17:103–111.
Gutierrez H, Dolcet X, Tolcos M, Davies A. 2004. HGF regulates the development of cortical pyramidal dendrites. Development. 131:3717–3726.
Hauser MD. 1996. The evolution of communication. Cambridge (MA): MIT Press.
Horton HL, Levitt P. 1988. A unique membrane protein is expressed on early developing limbic system axons and cortical targets. J Neurosci. 8:4653–4661.
Jackson PB, Boccuto L, Skinner C, Collins JS, Neri G, Gurrieri F, Schwartz CE. 2009. Further evidence that the rs1858830 C variant in the promoter region of the MET gene is associated with autistic disorder. Autism Res. 2:232–236.
Judson MC, Bergman MY, Campbell DB, Eagleson KL, Levitt P. 2009. Dynamic gene and protein expression patterns of the autism-associated met receptor tyrosine kinase in the developing mouse forebrain. J Comp Neurol. 513:511–531.
Judson MC, Eagleson KL, Wang L, Levitt P. 2010. Evidence of cell-nonautonomous changes in dendrite and dendritic spine morphology in the met-signaling-deficient mouse forebrain. J Comp Neurol. 518:4463–4478.
Just MA, Cherkassky VL, Keller TA, Minshew NJ. 2004. Cortical activation and synchronization during sentence comprehension in high-functioning autism: evidence of underconnectivity. Brain. 127:1811–1821.
Koshino H, Kana RK, Keller TA, Cherkassky VL, Minshew NJ, Just MA. 2008. fMRI investigation of working memory for faces in autism: visual coding and underconnectivity with frontal areas. Cereb Cortex. 18:289–300.
Langford DJ, Crager SE, Shehzad Z, Smith SB, Sotocinal SG, Levenstadt JS, Chanda ML, Levitin DJ, Mogil JS. 2006. Social modulation of pain as evidence for empathy in mice. Science. 312:1967–1970.
Lavenex P, Lavenex PB, Bennett JL, Amaral DG. 2009. Postmortem changes in the neuroanatomical characteristics of the primate brain: hippocampal formation. J Comp Neurol. 512:27–51.
Levy F. 2007. Theories of autism. Aust N Z J Psychiatry. 41:859–868.
MacLean PD. 1955. The limbic system ("visceral brain") and emotional behavior. Arch Neurol Psychiatry. 73:130–134.
Madhavan R, Peng HB. 2006. HGF induction of postsynaptic specializations at the neuromuscular junction. J Neurobiol. 66:134–147.
Malkova L, Mishkin M, Bachevalier J. 1995. Long-term effects of selective neonatal temporal lobe lesions on learning and memory in monkeys. Behav Neurosci. 109:212–226.
Marshall CR, Noor A, Vincent JB, Lionel AC, Feuk L, Skaug J, Shago M, Moessner R, Pinto D, Ren Y, et al. 2008. Structural variation of chromosomes in autism spectrum disorder. Am J Hum Genet. 82:477–488.
Nakano M, Takagi N, Takagi K, Funakoshi H, Matsumoto K, Nakamura T, Takeo S. 2007. Hepatocyte growth factor promotes the number of PSD-95 clusters in young hippocampal neurons. Exp Neurol. 207:195–202.
Nauta WJ. 1971. The problem of the frontal lobe: a reinterpretation. J Psychiatr Res. 8:167–187.
Ongur D, Price JL. 2000. The organization of networks within the orbital and medial prefrontal cortex of rats, monkeys and humans. Cereb Cortex. 10:206–219.
Papez JW. 1937. A proposed mechanism of emotion. Arch Neurol Psychiatry. 38:725–743.
Phelps EA, LeDoux JE. 2005. Contributions of the amygdala to emotion processing: from animal models to human behavior. Neuron. 48:175–187.
Pimenta AF, Reinoso BS, Levitt P. 1996. Expression of the mRNAs encoding the limbic system-associated membrane protein (LAMP): II. Fetal rat brain. J Comp Neurol. 375:289–302.
Pinsk MA, Arcaro M, Weiner KS, Kalkus JF, Inati SJ, Gross CG, Kastner S. 2009. Neural representations of faces and body parts in macaque and human cortex: a comparative FMRI study. J Neurophysiol. 101:2581–2600.
Pinsk MA, DeSimone K, Moore T, Gross CG, Kastner S. 2005. Representations of faces and body parts in macaque temporal cortex: a functional MRI study. Proc Natl Acad Sci U S A. 102:6996–7001.
Rakic P. 1974. Neurons in rhesus monkey visual cortex: systematic relation between time of origin and eventual disposition. Science. 183:425–427.
Romanski LM, Giguere M, Bates JF, Goldman-Rakic PS. 1997. Topographic organization of medial pulvinar connections with the prefrontal cortex in the rhesus monkey. J Comp Neurol. 379:313–332.
Sanchez-Andrade G, James BM, Kendrick KM. 2005. Neural encoding of olfactory recognition memory. J Reprod Dev. 51:547–558.
Shipp S. 2003. The functional logic of cortico-pulvinar connections. Philos Trans R Soc Lond B Biol Sci. 358:1605–1624.
Sousa I, Clark TG, Toma C, Kobayashi K, Choma M, Holt R, Sykes NH, Lamb JA, Bailey AJ, Battaglia A, et al. 2009. MET and autism susceptibility: family and case-control studies. Eur J Hum Genet. 17:749–758.
Spehr M, Kelliher KR, Li XH, Boehm T, Leinders-Zufall T, Zufall F. 2006. Essential role of the main olfactory system in social recognition of major histocompatibility complex peptide ligands. J Neurosci. 26:1961–1970.
Steckler T, Drinkenburg WH, Sahgal A, Aggleton JP. 1998. Recognition memory in rats–II. Neuroanatomical substrates. Prog Neurobiol. 54:313–332.
Stefanacci L, Amaral DG. 2002. Some observations on cortical inputs to the macaque monkey amygdala: an anterograde tracing study. J Comp Neurol. 451:301–323.
Stefanacci L, Suzuki WA, Amaral DG. 1996. Organization of connections between the amygdaloid complex and the perirhinal and parahippocampal cortices in macaque monkeys. J Comp Neurol. 375:552–582.
St John RD. 1973. Genetic analysis of tail rattling in the mouse. Nature. 241:549–551.
Swanson LW, Petrovich GD. 1998. What is the amygdala? Trends Neurosci. 21:323–331.
Thornton JA, Rothblat LA, Murray EA. 1997. Rhinal cortex removal produces amnesia for preoperatively learned discrimination

problems but fails to disrupt postoperative acquisition and retention in rhesus monkeys. J Neurosci. 17:8536–8549.
Tsao DY, Freiwald WA, Tootell RB, Livingstone MS. 2006. A cortical region consisting entirely of face-selective cells. Science. 311:670–674.
Tsao DY, Livingstone MS. 2008. Mechanisms of face perception. Annu Rev Neurosci. 31:411–437.
Tyndall SJ, Walikonis RS. 2006. The receptor tyrosine kinase Met and its ligand hepatocyte growth factor are clustered at excitatory synapses and can enhance clustering of synaptic proteins. Cell Cycle. 5:1560–1568.
Wyss JM, Sripanidkulchai K. 1983. The indusium griseum and anterior hippocampal continuation in the rat. J Comp Neurol. 219:251–272.
Yeterian EH, Pandya DN. 1997. Corticothalamic connections of extrastriate visual areas in rhesus monkeys. J Comp Neurol. 378:562–585.